Gene Expression–Based Molecular Test as Diagnostic Aid for the Differential Diagnosis of Psoriasis and Eczema in Formalin-Fixed and Paraffin-Embedded Tissue, Microbiopsies, and Tape Strips

JID Open

Felix Fischer[1,12], Anais Doll[2,12], Deniz Uereyener[1], Sophie Roenneberg[2], Christina Hillig[1], Lucca Weber[3], Verena Hackert[3], Martin Meinel[1], Ali Farnoud[1], Peter Seiringer[2], Jenny Thomas[7], Philipp Anand[2], Larissa Graner[5], Franziska Schlenker[5], Roland Zengerle[4,5], Pontus Jonsson[6], Manja Jargosch[2,7], Fabian J. Theis[1,8], Carsten B. Schmidt-Weber[7], Tilo Biedermann[2], Michael Howell[9], Kristian Reich[10], Kilian Eyerich[11], Michael Menden[1], Natalie Garzorz-Stark[2], Felix Lauffer[2,12] and Stefanie Eyerich[7,12]

Highly effective targeted therapies are available to treat noncommunicable chronic inflammatory skin diseases. In contrast, the exact diagnosis of noncommunicable chronic inflammatory skin diseases is complicated by its complex pathogenesis and clinical and histological overlap. Particularly, the differential diagnosis of psoriasis and eczema can be challenging in some cases, and molecular diagnostic tools need to be developed to support a gold standard diagnosis. The aim of this work was to develop a real-time PCR-based molecular classifier to distinguish psoriasis from eczema in formalin-fixed and paraffin-embedded-fixed skin samples and to evaluate the use of minimally invasive microbiopsies and tape strips for molecular diagnosis. In this study, we present a formalin-fixed and paraffin-embedded–based molecular classifier that determines the probability for psoriasis with a sensitivity/specificity of 92%/100%, respectively, and an area under the curve of 0.97, delivering comparable results to our previous published RNAprotect-based molecular classifier. The psoriasis probability, as well as levels of *NOS2* expression, positively correlated with the disease hallmarks of psoriasis and negatively with eczema hallmarks. Furthermore, minimally invasive tape strips and microbiopsies were effectively used to differentiate psoriasis from eczema. In summary, the molecular classifier offers broad usage in pathology laboratories as well as outpatient settings and can support the differential diagnosis of noncommunicable chronic inflammatory skin diseases on a molecular level using formalin-fixed and paraffin-embedded tissue, microbiopsies, and tape strips.

Journal of Investigative Dermatology (2023) **143,** 1461–1469; doi:10.1016/j.jid.2023.02.015

INTRODUCTION

Psoriasis and eczema are among the most prevalent and relevant skin diseases worldwide, with an incidence rate for both diseases together of at least 2% (Bylund et al., 2020; Thyssen et al., 2010; Vena et al., 2010). Although more than a dozen immune-modulating therapies, particularly mAbs targeting specific cytokines or their receptors, have been made available over the past decade, allowing a highly effective treatment of affected patients (Tizek et al., 2022), the ultimate breakthrough would include the development of accurate diagnostic tools. Diagnosis of both diseases largely depends on a subjective visual examination and histopathologic examination. Because of phenotypical overlaps of both diseases, up to 50% of cases with a palmoplantar localization are misdiagnosed (Kolesnik et al., 2018). To close this important diagnostic gap, a gene expression–based classifier using *NOS2* and *CCL27* as marker genes has been proposed, and its clinical validity has been examined and proven in various patient cohorts (Bentz et al., 2021; Brunner et al., 2019; Garzorz-Stark et al., 2016; Quaranta et al., 2014; Stoffel et al., 2018). Renert-Yuval et al. (2021) list the

[1]*Institute of Computational Biology, Helmholtz Center Munich, Neuherberg, Germany;* [2]*Department of Dermatology and Allergy, Technical University of Munich, Munich, Germany;* [3]*Dermagnostix GmbH, Freiburg, Germany;* [4]*Laboratory for MEMS Applications, Department of Microsystems Engineering – IMTEK, University of Freiburg, Freiburg, Germany;* [5]*Hahn-Schickard, Freiburg, Germany;* [6]*Karolinska Universitetssjukhuset - Hudkliniken Stockholm, Stockholm, Sweden;* [7]*ZAUM–Center of Allergy and Environment, Technical University of Munich and Helmholtz Center Munich, Munich, Germany;* [8]*Department of Mathematics, Technical University of Munich, Garching, Germany;* [9]*DermTech, San Diego, California, USA;* [10]*Translational Research in Inflammatory Skin Diseases, University Medical Center Hamburg-Eppendorf, Hamburg, Germany; and* [11]*Klinik für Dermatologie und Venerologie, Universitätsklinikum Freiburg, Freiburg, Germany*

[12]*These authors contributed equally to this work.*

Correspondence: Stefanie Eyerich, ZAUM - Center of Allergy and Environment, Technische Universität and Helmholtz Center Munich. Biedersteinerstr. 29, Munich 80802, Germany. E-mail: stefanie.eyerich@tum.de

Abbreviations: AD, atopic dermatitis; FFPE, formalin-fixed and paraffin-embedded; MC, molecular classifier; RNA-seq, RNA sequencing

Received 20 October 2022; revised 28 January 2023; accepted 14 February 2023; accepted manuscript published online 7 March 2023; corrected proof published online 3 April 2023

© 2023 The Authors. Published by Elsevier, Inc. on behalf of the Society for Investigative Dermatology. This is an open access article under the CC BY-NC-ND license (http://creativecommons.org/licenses/by-nc-nd/4.0/).

NOS2/CCL27 classifier as the only accepted disease classifier for psoriasis and eczema. As the previous molecular classifier (MC) was developed with RNAprotect-fixed biopsies, we here investigated if the MC could be transferred to formalin-fixed and paraffin-embedded (FFPE) skin samples that are widely used for diagnostic measures in pathology laboratories and if the MC could be applied to minimally invasive methods such as microbiopsies and tape strips. We show that an FFPE-based MC delivers the correct clinical and histopathologic diagnosis at the level of RT-PCR with a test sensitivity and specificity of 92% and 100%, respectively. We further applied the MC successfully to minimally invasive microbiopsies and pointed out the potential use of tape strips for molecular diagnosis, highlighting the application of the MC to any non- and minimally invasive sample collection and allowing application in routine diagnostics to aid physicians in differentiating psoriasis from eczema.

RESULTS

The FFPE-based MC precisely separates eczema from psoriasis and efficiently identifies subtypes of both diseases

To evaluate the potential of FFPE samples for molecular diagnostics, 77 FFPE samples of lesional psoriasis (n = 27) and eczema (atopic dermatitis [AD], n = 29; nummular eczema, n = 21) were analyzed by probe-based real-time PCR for the expression of *NOS2* and *CCL27*. The diagnosis of patients was performed by two independent dermatologists who evaluated the clinical picture, family history, laboratory parameters, and histological hallmarks of each patient. To calculate an FFPE-based MC for the differentiation of psoriasis and eczema, a logistic regression model was fitted with a 5-times cross-validation with random subsampling. This classifier was designed to predict the probability of psoriasis with a cutoff value of 55% (the range between 45% and 55% does result in a probability at which samples are regarded as undetermined).

Two patients with diagnosed psoriasis were misclassified by the MC as patients with eczema, and two further patients with psoriasis reached a probability between 45% and 55% and thereby were regarded as undetermined. The model achieved a test specificity for psoriasis of 100%, with a sensitivity of 92%, and an area under the receiver operating characteristic curve of 0.97 ± 0.06 if undetermined patients were not included (Figure 1a-c) and a specificity of 91% and sensitivity of 87% if they were included. In the next step, we used the FFPE-based MC to classify subtypes of psoriasis (psoriasis guttata, n = 5; psoriasis palmoplantaris, n = 1; generalized pustular psoriasis, n = 2; and psoriasis pustulosa palmoplantaris, n = 3) and eczema (dyshidrotic eczema, n = 4; hyperkeratotic-rhagadiform eczema, n = 3) (Figure 1d). Although all cases of psoriasis guttata, psoriasis palmoplantaris, and psoriasis pustulosa palmoplantaris were diagnosed correctly by the FFPE-based MC, cases of dyshidrotic and hyperkeratotic-rhagadiform eczema as well as generalized pustular psoriasis tended to be misdiagnosed.

FFPE classifier results correlate with clinical attributes of psoriasis and eczema and support diagnostic decision-making in patients with inconsistent diagnosis

To understand if the determined probability for psoriasis correlates with clinical attributes associated with psoriasis or eczema, Pearson correlation coefficients were determined (Figure 1e). The probability of psoriasis positively correlated with the histologic attributes dilated dermal capillaries ($r = 0.61$, $P = 0.000038$), acanthosis ($r = 0.51$, $P = 0.00079$), neutrophils ($r = 0.39$, $P = 0.015$), and parakeratosis ($r = 0.33$, $P = 0.039$) (Figure 1e)—all hallmarks of the pathogenesis of psoriasis. This positive correlation was followed by a significant positive correlation of negative Ct values of *NOS2* (dilated dermal capillaries, $r = 0.43$, $P = 0.0062$; acanthosis, $r = 0.33$, $P = 0.043$) and a significant negative correlation with negative delta Ct values for *CCL27* (dilated dermal capillaries, $r = -0.54$, $P = 0.00042$; acanthosis, $r = -0.5$, $P = 0.00052$; neutrophils, $r = -0.48$, $P = 0.0018$). In line, the probability of psoriasis and the negative delta Ct for *NOS2* showed a significant positive correlation with a psoriasis type morphology ($r = 0.77$, $P = 0.00000024$, and $r = 0.56$, $P = 0.00098$) and a trend of positive correlation with arthritis ($r = 0.34$, $P = 0.056$, and $r = 0.35$, $P = 0.41$), whereas a significant negative correlation was determined for an eczema type morphology ($r = -0.77$, $P = 0.00000024$, and $r = -0.56$, $P = 0.00098$) and rhinoconjunctivitis allergica ($r = -0.47$, $P = 0.0054$ and $r = -0.28$, $P = 0.12$) (Figure 1e). The probability of psoriasis also showed a trend of positive correlation with the therapeutic efficiency of IL12/IL-23 ($r = 0.99$, $P = 0.056$) and TNF-a inhibition ($r = 0.56$, $P = 0.15$), and a trend of negative correlation with the response to fumarate ($r = -0.34$, $P = 0.37$). No correlations of the laboratory parameters *Staphylococcus aureus* and specific IgE or with the family history of for psoriasis and eczema were identified.

To further evaluate the potential of the FFPE-based MC to support diagnostic decision-making, 14 patient samples with discrepant clinical and histologic diagnoses were analyzed. Within this cohort, nine patients were assigned a probability for psoriasis and five patients were classified as eczema (Supplementary Figure S1a). Follow-up of these patients after therapy initiation revealed a concordance of the MC result and the therapeutic efficiency (see Supplementary Materials and Methods on selected cases; Supplementary Figure S1).

The MC is equally efficient in minimally invasive microbiopsies

Next, we investigated whether the MC can also be useful for correctly diagnosing psoriasis or atopic eczema using microbiopsies (Ø1 mm). The advantages of microbiopsies are the unnecessity of local anesthesia and the almost invisible scar, whereas all layers of the skin, including subcutaneous fat, can be captured. We established a cohort of patients receiving conventional 4−6 mm biopsies as well as 1-mm microbiopsies from the same psoriasis (n = 37) or AD (n = 46) lesion. Five pairs of psoriasis macrobiopsies and microbiopsies as well as five pairs of ADs were analyzed by RNA sequencing (RNA-seq). As expected, macrobiopsies showed a clustering of psoriasis or AD biopsies in principal component analysis, as well as an upregulation of disease-specific genes, such as *IL17*, *NOS2*, and *DEFB4* in psoriasis samples and *IL13*, *CCL27*, and *NELL2* in AD, respectively (Figure 2b−d and Supplementary Table S1). RNA-seq analysis of microbiopsies led to concordant results: disease-specific clusters in principal component analysis and upregulation

of disease-characteristic genes, thus confirming that microbiopsies are as useful as conventional biopsies to detect gene regulations in the skin (Figure 2e–g and Supplementary Table S1). To test if microbiopsies are also adequate tissue samples for the MC, we analyzed *NOS2* and *CCL27* gene expression in 83 pairs of macro- and microbiopsies by RT-PCR. Delta Ct values showed no significant difference between macro- and microbiopsies. In line with our experience from previous studies, we detected high *NOS2* expression in psoriasis and high *CCL27* expression in atopic eczema (Figure 2h). Finally, the MC was run for all samples of the macro- and microbiopsy cohort. The probability for psoriasis or eczema was comparable between 76 of 83 samples. Although the MC misclassified one patient in the macrobiopsy cohort (0.83%), six patients (4.98%) were misclassified by microbiopsies (Figure 2i). Thus, although the MC led to reliable results in most of the samples (91.57%) independent of the size of the biopsy, there is a small increase in misclassification in the microbiopsy cohort.

Tape strips of inflamed epidermis can be utilized for molecular diagnostics

Minimally invasive methods for diagnostic purposes are highly desirable. Therefore, we tested the potential use of tape strips for molecular diagnosis of psoriasis and eczema. After the application of the tape strips to inflamed skin (AD: n = 10, psoriasis: n = 11; Figure 3a), total RNA was isolated and real-time PCR was performed with the same reagents used for FFPE samples. Whereas median delta Ct values for *CCL27* did not differ between FFPE and tape strip samples as well as the disease, significant differences were observed for *NOS2* (AD: $P = 0.0001$, psoriasis: $P = 0.011$) (Figure 3b). This might be because of the small cohort of tape-stripping patients and the fact that *NOS2* is highly regulated during inflammation. Nevertheless, FFPE and tape strip delta Ct values of *NOS2* are significantly different between AD and psoriasis, highlighting again the value of this combination of markers for molecular diagnostics (Supplementary Table S1). Because of the sample size, no tape-specific MC was calculated. However, the delta Ct values of *NOS2* and *CCL27* efficiently separate psoriasis from AD samples (Figure 3c). In this study, one psoriasis sample was misdiagnosed. Further investigation showed that this patient was not affected by psoriasis, but pityriasis rubra pilaris.

DISCUSSION

The development of highly specific biologic drugs has revolutionized treatment options for various diseases during the past two decades (Noda et al., 2015). However, owing to their high specificity for one or two proinflammatory mediators, these drugs are highly effective only in selected diseases and patients calling for stringent diagnosis and subsequent assignment of each patient to the most appropriate drug. However, diagnosis of psoriasis and eczema can be challenging at the hands, feet, and scalp, and 12.8% (in our cohort) up to 50% (Kolesnik et al., 2018) of patients are estimated to be misdiagnosed. Although molecular diagnostics have already been adopted in various cancers to optimize diagnosis and selection of treatment regimens, they are not well established in the management of chronic inflammatory skin diseases yet (Grazia et al., 2014; Levine and Fisher, 2014; Usher-Smith et al., 2014). In previous work, we have developed a disease classifier to more precisely distinguish psoriasis from eczema based on the expression levels of *NOS2* and *CCL27* (Garzorz-Stark et al., 2016; Quaranta et al., 2014). This classifier has subsequently been validated by several groups and obtained acceptance as a molecular tool to differentiate these two common skin conditions (Bentz et al., 2021; Brunner et al., 2019; Stoffel et al., 2018). However, it was established on RNA-protected fixed skin that is regularly used in research but not in routine clinical practice or at pathology laboratories, where skin samples are usually FFPE. This method of fixation allows for long-term storage of samples and optimal assessment of histologic hallmarks; however, owing to the cross-linking of proteins with RNA and the resulting RNA degradation because of the fixation procedure, RNA isolation from FFPE samples can be challenging. In this study, optimized protocols have been developed to minimize the negative effects of the fixation method, which now allows usage of this sample type for molecular diagnostics. Within this work, we have transferred the RNAprotect-based MC to FFPE samples and were able to produce comparable results. The RNAprotect-based MC distinguished psoriasis from eczema with a sensitivity and specificity for psoriasis of 97.7% and 100%, respectively, and an area under the curve of 0.99, whereas the FFPE-based classifier determined probabilities for psoriasis with a sensitivity and specificity and of 92% and 100%, respectively, and an area under the curve of 0.97 (Garzorz-Stark et al., 2016). Only 2 of 27 classical psoriasis samples were misclassified by the FFPE-based MC, and all AD and nummular eczema cases were correctly diagnosed. The FFPE-based MC was also able to predict the diagnosis of psoriasis subtypes; however, it delivered conflicting results for dyshidrotic and hyperkeratotic-rhagadiform eczema. Unfortunately, the cohorts of these subtypes were very small (4 and 3 cases, respectively), and data on treatment regimens and treatment responses were not available. Because these patients are difficult to diagnose by current gold standard diagnostics, further studies are needed to monitor treatment response after diagnostic decision-making to understand the potential superiority of molecular classification compared with current diagnostic measures in these eczema subtypes and patients with discrepant clinical and histologic diagnosis.

In line with previous findings, the FFPE-based classifier probability was highly correlated with disease hallmarks of psoriasis, but not hallmarks of eczema (Garzorz-Stark et al., 2016). Thus, the reliability of the two markers *NOS2* and *CCL27* has now also been shown in FFPE tissue, facilitating the possible implementation of this molecular diagnostic aid in routine clinical practice and pathology laboratories. Minimally invasive diagnostic tools need to be developed to reduce trauma and enhance acceptance by patients (Hadeler et al., 2021). In this study, we could show that the gene expression profiles of macrobiopsies are adequately reflected in microbiopsies and that analysis of these small biopsies delivers comparable MC results. However, approximately 5% of patients were misclassified based on microbiopsies, especially psoriasis cases, which were incorrectly classified as eczema. The values for the delta Ct of *NOS2* were significantly different between incorrectly classified and

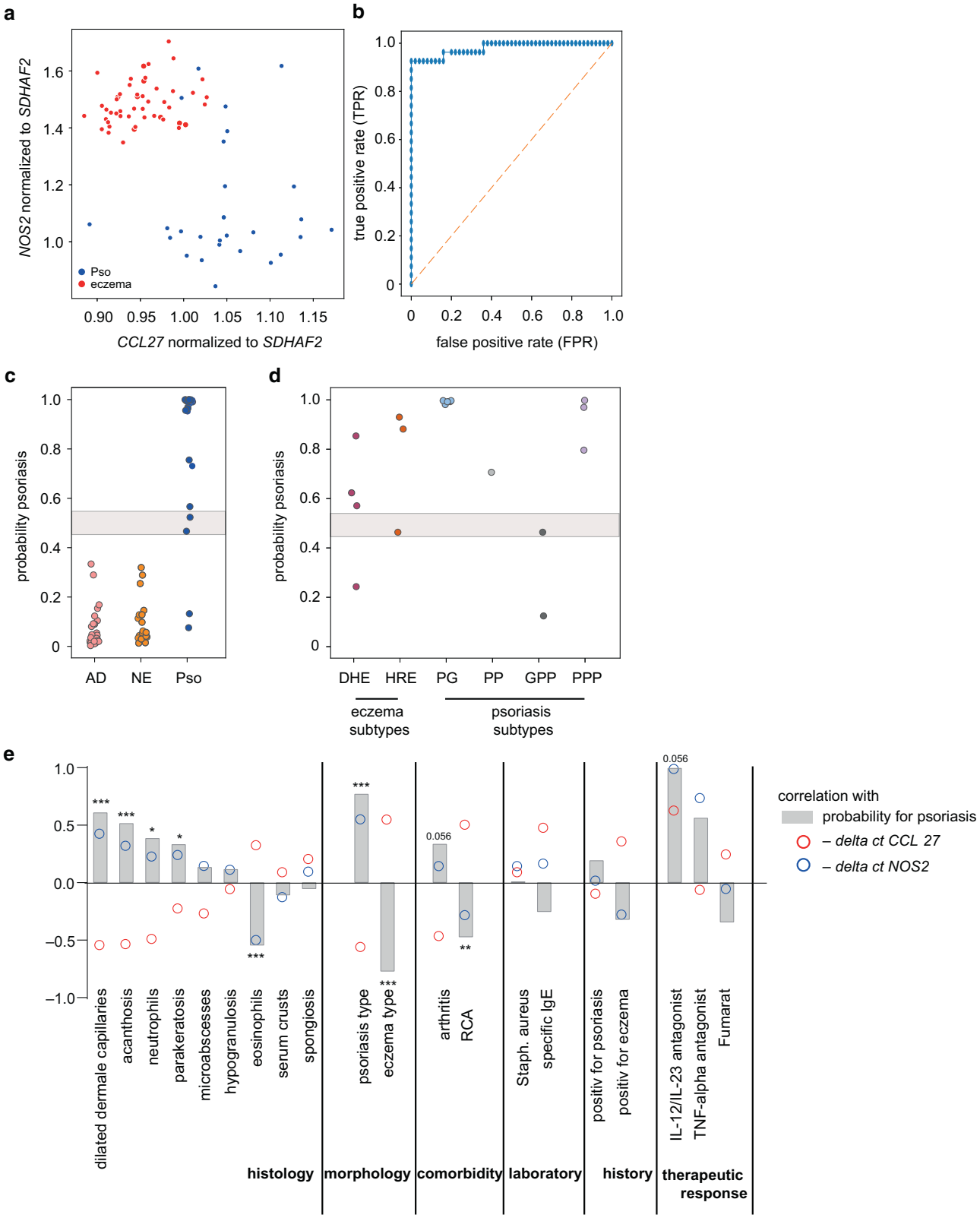


Figure 1. The FFPE-based MC dissects clinically clear cases of psoriasis and eczema, is efficient in subtypes of both diseases, and correlates with clinical disease hallmarks. (**a**) The MC was trained on clear cases of eczema (AD, n = 29; NE, n = 21; Pso, n = 27) using a logistic regression model with a 5-fold cross-validation delivering the probability of psoriasis. Ct values of *NOS2* and *CCL27* were normalized to the reference genes *SDHAF2* and *TBP* (not shown). (**b**) Sensitivity and specificity of the MC. (**c**) FFPE-based MC determined probabilities for psoriasis in clear cases of AD, NE, and Pso. The gray area between 45% and 55% indicates undetermined probabilities. (**d**) Probability prediction for psoriasis in subtypes of eczema and psoriasis (DHE, n = 4; HRE, n = 3; PG, n = 5; PP, n = 1; GPP, n = 2; PPP, n = 2). A probability between 45% and 55% was defined as not evaluable. (**e**) Pearson correlation of probability for psoriasis as well as negative delta Ct values for *CCL27* and *NOS2* with clinical attributes. Stars indicate the significance of the probability of psoriasis with clinical attributes.

correctly classified patients with psoriasis, whereas the delta Ct values of *CCL27* were comparable. One possible explanation is that the smaller size of the biopsy does not allow optimal detection of the full inflammatory repertoire. The analysis of two microbiopsies instead of just one might overcome this limitation. Microbiopsies are currently also being evaluated as a potential source for diagnostic procedures in infectious or autoinflammatory skin diseases (Churiso et al., 2020; Yamada et al., 2021), which will generate further evidence regarding their diagnostic potential across various skin conditions.

We have also investigated tape stripping as a minimally invasive sampling method for molecular diagnostics and showed an adequate distinction between psoriasis and eczema based on the expression of *NOS2* and *CCL27* in tape strip-derived sample material. Because the tape strip analysis was performed as a proof of concept in a small cohort, no MC has been calculated yet. Our findings corroborate the results of a recent study that described the gene expression profiling of tape strip–derived samples from skin lesions of psoriasis and eczema by RNA-seq and indicated the potential use of *NOS2* to discriminate between both diseases (He et al., 2021). Because of the minimally invasive sampling procedure, tape stripping may be particularly useful for the testing of visible and sensitive skin areas and in children, as well as for repetitive sampling procedures necessary to monitor treatment responses over time (Andersson et al., 2022; Mikhaylov et al., 2021; Poh et al., 2022). However, in contrast to macro- or microbiopsies, tape stripping primarily samples epidermal cells and may have limited detection power with regard to dermal changes as long as these are not accompanied by characteristic deviations from epidermal pathways.

In summary, we show that our MC for discriminating psoriasis from eczema produces meaningful results in a broad range of skin tissue derived from invasive to minimally invasive sampling techniques. Further efforts are required to simplify and shorten the labor- and cost-intensive procedures of RNA isolation and real-time PCR. One possible solution is a fully automated and closed system, which would also allow the integration of molecular diagnostics into routine patient management at the point of care.

MATERIALS AND METHODS

Patient cohorts

Skin samples were collected for three different cohorts: (i) FFPE samples (<10 years of age) for a retrospective study were derived from the Biobank Biederstein and consisted of 109 patients (psoriasis, n = 27; eczema, n = 50; disease subtypes, n = 18 [psoriasis guttata, n = 5; psoriasis palmoplantaris, n = 1; generalized pustular psoriasis, n = 2; psoriasis pustulosa palmoplantaris, n = 3; dyshidrotic eczema, n = 4; hyperkeratotic rhagadiforme eczema, n = 3], and cases with contradictory diagnosis, n = 14) (Table 1), (ii) pairs of macrobiopsies (diameter of 4–6 mm) and microbiopsies (diameter of 1 mm) from the same skin lesion were collected from patients with psoriasis (n = 37) and AD (n = 46), (iii) minimally invasive tape strips ('Smart Stickers', DermTech, San Diego, CA) were collected from skin lesions of patients with psoriasis (n = 11) and AD (n = 10). The final diagnosis of all patients was determined by at least two dermatologists taking a comprehensive view of the clinical picture, family history, laboratory parameters, and histological assessment. All patients gave written informed consent, and the study was approved by the local ethical committee of the Klinikum rechts der Isar, Technical University Munich (project numbers 2773/10 and 515/17).

Patient material sampling and isolation of RNA

Skin biopsies (Ø3–6 mm) for cohort 1 were immediately fixed in neutral buffered formalin for 8 to 48 hours at room temperature or 4 °C. Fixed biopsies were paraffin-embedded according to standard procedures (one biopsy per paraffin cassette). Unstained FFPE skin biopsies were used to isolate mRNA. In this study, tissue sections with a thickness of 10 μm were generated from each FFPE skin sample. The first sections containing both epidermis and dermis were trimmed (at least 30 μM) and discarded to avoid the use of degraded material. mRNA was extracted from a total of three FFPE sections using a magnetic bead-based purification method according to the manufacturer's protocol (InnuPREP MP Basic FFPE RNA Kit, IST Innuscreen, Berlin, Germany). The mRNA eluates were analyzed immediately after the extraction by real-time PCR.

For cohort 2, macrobiopsies were taken under local anesthesia and sutured, whereas microbiopsies did not need anesthesia or suture. Macro- and microbiopsies were fixed in RNAprotect tissue reagent (Qiagen, Germantown, MD), incubated for 24 to 48 hours at 4 °C, and stored at −20 °C. For RNA isolation, RNAprotect-fixed macrobiopsies and microbiopsies were cut into pieces and homogenized using a steel bead in a Tissue Lyzer (Qiagen) for two rounds of 5 minutes each at 23 Hz. mRNA was subsequently isolated from homogenates using the mRNeasy Mini Kit (Qiagen), according to manufacturer's procedure. The mRNA eluates were either analyzed immediately after the extraction by real-time PCR/RNA-seq or stored at −80 °C until analysis.

Minimally invasive tape strips for cohort 3 were applied to skin lesions, softly pressed and rubbed before lifting, and kept for a maximum of 7 days at room temperature before analysis. Total RNA from tape strips was isolated using the InnuPREP MP Basic FFPE RNA Kit (Innuscreen) without the decrosslinking incubation at 80 °C. Isolated total RNA was immediately used for real-time PCR analysis.

Real-time PCR

Specific primers were designed using the primer design tool PrimerBLAST from NCBI (www.ncbi.nlm.nih.gov/tools/primer-blast/). Primers and hydrolysis probes were obtained from Biomers (Baden-Württemberg, Germany). Probes were labeled with an Atto 647N fluorophore at the 5′-end and quenched with a BHQ2 quencher at the 3′-end. Supplementary Table S3 gives an overview of all used primers, hydrolysis probes, and methods to transcribe cDNA. For FFPE samples and tape strips, real-time PCR reactions were carried out in 96-well plates using a Thermo Fisher Scientific (Waltham, MA) one-step RT-PCR master mix. Thermocycling and fluorescence detection were performed in a qTower^3 (Analytik Jena, Germany), and amplification results were analyzed using the qPCRsoft 4.1 software (Analytik). For macrobiopsies and microbiopsies, real-time

Significance was defined as $*P < 0.05$; $**P < 0.01$; $***P < 0.001$. AD, atopic dermatitis; DHE, dyshidrotic eczema; FFPE, formalin-fixed and paraffin-embedded; GPP, generalized pustular psoriasis; HRE, hyperkeratotic-rhagadiform eczema; MC, molecular classifier; NE, nummular eczema; PG, psoriasis guttata; PP, psoriasis palmoplantaris; PPP, psoriasis pustulosa palmoplantaris; Pso, psoriasis; RCA, rhinoconjunctivitis allergica.

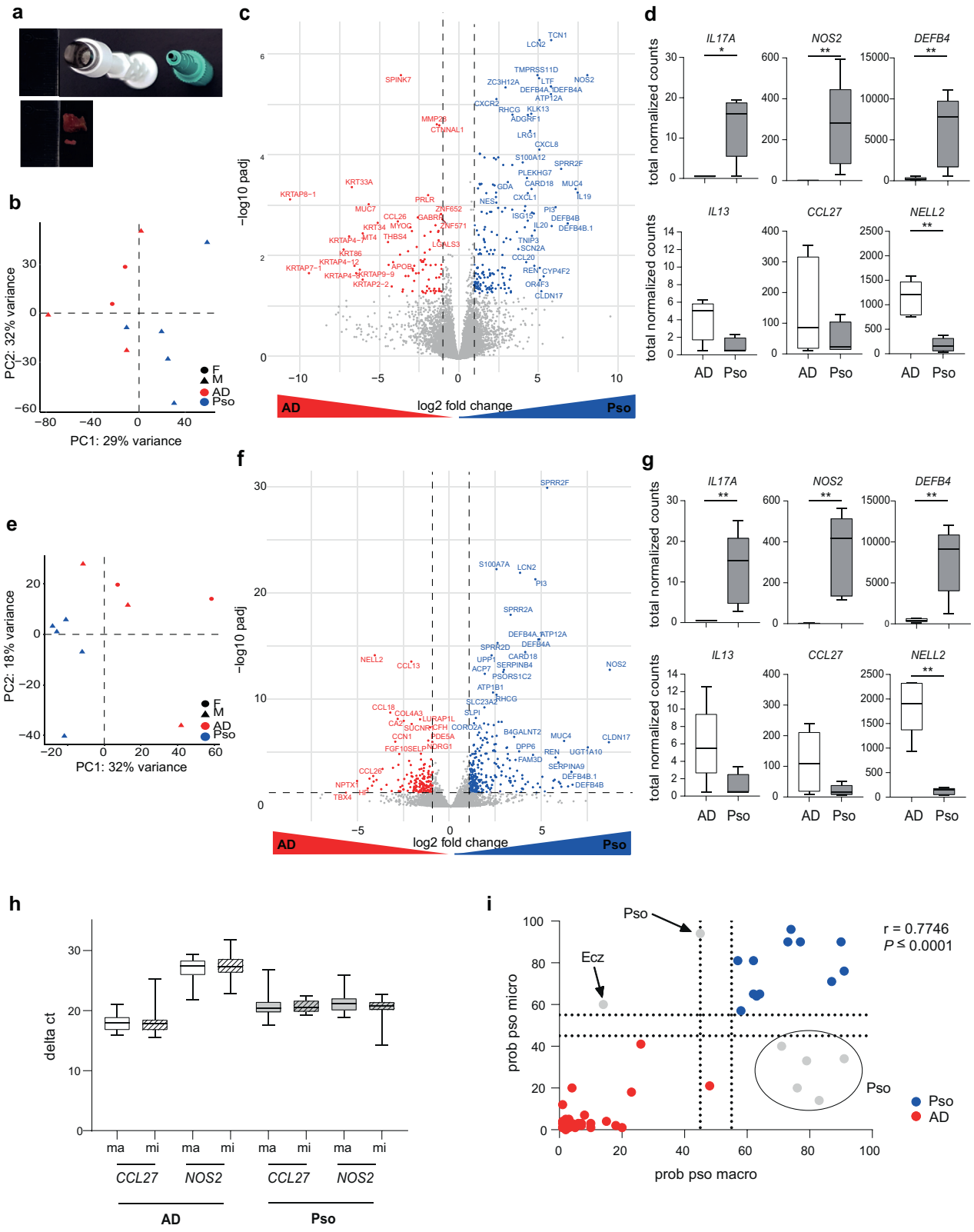


Figure 2. Micro- and macrobiopsies show comparable gene expression profiles enabling the use of microbiopsies for molecular diagnosis. (**a**) Comparison of invasive Ø6-mm punch (macro) biopsies and minimally invasive Ø1 mm microbiopsies. (**b**) PCA analysis of the macrobiopsy cohort (Pso, n = 5; AD, n = 5). (**c**) Volcano plot of significantly regulated genes (*P*adj < 0.05, log2foldchange > 1) in macrobiopsies determined by RNA sequencing. (**d**) Hallmark genes for AD (white) and Pso (gray) pathogenesis in macrobiopsies. Significance were determined by Mann-Whitney *U* test (**P* < 0.05; ***P* < 0.01) (**e**) PCA of the corresponding microbiopsy cohort (Pso, n = 5; AD, n = 5). (**f**) Volcano plot of significantly regulated genes (*P*adj < 0.05, log2foldchange > 1) in microbiopsies determined by RNA sequencing. (**g**) Hallmark genes for AD (white) and Pso (gray) pathogenesis in microbiopsies. Significance was determined by the Mann-Whitney *U* test (**P* < 0.05; ***P* < 0.01). (**h**) The delta Ct values for *NOS2* and *CCL27* normalized to 18*S* expression for macro- and microbiopsy samples in AD

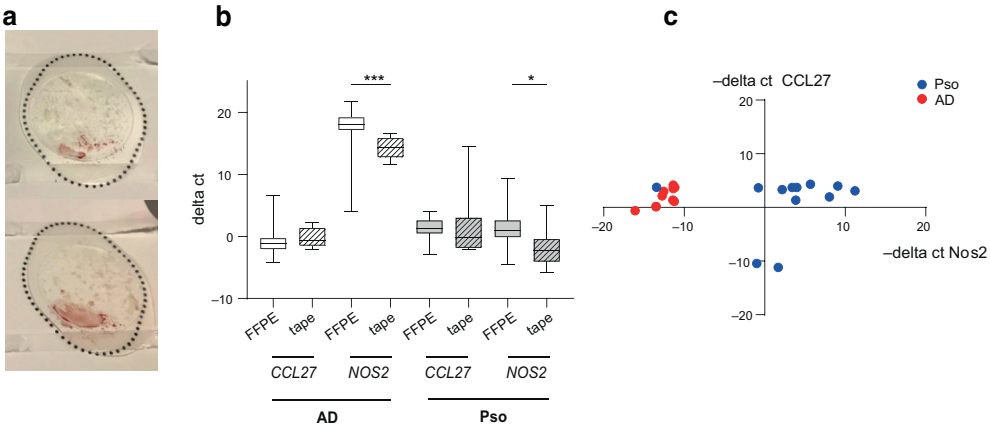


Figure 3. Minimally invasive tape strips efficiently discriminate psoriasis from eczema. (**a**) A tape strip of human skin illustrating skin cells sticking to the tape. (**b**) Delta Ct values for *NOS2* and *CCL27* normalized to *SDHAF2* expression for FFPE samples and tape strips in AD (n = 48 and n = 11, respectively) and Pso (n = 27 and n = 11, respectively) samples. Statistical significance was determined using one-way ANOVA and the Tukey's multiple comparisons test (*$P < 0.05$; **$P < 0.01$; ***$P < 0.001$). All determined significances are given in Supplementary Table S2b. (**c**) Delta Ct values for *NOS2* and *CCL27* shown for each single tape strip patient (Pso, n = 10 [blue]; AD, n = 11 [red]). Higher delta Ct values represent lower expression. AD, atopic dermatitis; FFPE, formalin-fixed and paraffin-embedded; Pso, psoriasis.

PCR was performed in 384-well plates using the Fast Start Universal SYBRGreen Master (Rox) (Roche Life Science, Basel, Switzerland) on a ViiA TM 7 Real-Time PCR System (Applied Biosystems, Waltham, MA). cDNA synthesis was performed with the High-Capacity cDNA Reverse Transcription Kit (Life Technologies, Carlsbad, CA) according to the manufacturer's instructions (Supplementary Table S3).

RNA-seq and RNA-seq analysis

Purified mRNA from macro- and microbiopsy pairs (n = 10) was subjected to RNA-seq. RNA-seq libraries were generated using the TruSeq Stranded Total RNA Kit (Illumina) according to the manufacturer's high sample protocol and sequenced on an Illumina HiSeq4000 as paired-end with a read length of 2 × 150 base pair and an average output of 40 Mio reads per sample.

The comparison of AD and psoriasis samples was performed separately for macrobiopsies and microbiopsies. The differential gene expression analyses were conducted using the DESeq2 package from Bioconductor (www.bioconductor.org). Gene counts were normalized with a variance stabilizing transformation. Only protein-coding genes that have total counts of more than one were included in the analyses. In addition, all uncharacterized genes, Y chromosome–related genes, and pseudogenes were filtered out. The design of both, the macro- and microbiopsies differential gene expression analyses were $\sim 0 + Age + Sex + Diagnosis$, where *Diagnosis* is either AD or psoriasis. The threshold determining the significance for differentially expressed genes was adjusted *P* values < 0.05 according to Benjamini and Hochberg, and the absolute log2 fold change ≥1.

FFPE-based MC built-up

The FFPE-based MC predicts the disease state (probability for psoriasis) directly from the normalized Ct values of *NOS2* and *CCL27* normalized to the reference genes *SDHAF2* and *TBP* and classifies a sample according to the molecular signature of psoriasis versus the one of eczema. The FFPE-based MC was built using L2 regularized logistic regression. L2 regularization was used to avoid numerical artifacts, and regularization strength was increased until the different signs' effect was only very weak or gone. For classification, the psoriasis and eczema subtypes are aggregated into their respective high-level labels (eczema or psoriasis). The model was fitted using the LogisticRegression implementation from Scikit-Learn with an L2 regularization strength of 100. In addition, the uncertainty of the model is estimated based on the predicted probability (cases with a predicted probability between 45% and 55% are predicted as undetermined). The model was trained on 77 patients with a clear diagnosis of psoriasis and eczema (AD and nummular eczema) and evaluated on the training data plus 18 additional patients with prediagnosed subtypes of psoriasis and eczema.

For the analysis of macrobiopsies and microbiopsies, our previously RNAprotect-based MC was used (Garzorz-Stark et al., 2016; Quaranta et al., 2014).

Correlation of FFPE-based MC probability and PCR results with clinical attributes

Pearson correlation coefficients were calculated to determine the correlation between the FFPE-based MC determined probabilities for psoriasis, the negative delta Ct PCR results of *CCL27* and *NOS2*, as well as histologic parameters, the morphology of the lesion, comorbidities, laboratory parameters, and family history.

Statistical analysis

Statistical analysis was performed using GraphPad Prism 9.3 (GraphPad Software, Boston, MA). For multiple comparisons, one-way ANOVA with Tukey's multiple comparison test was used. For single comparisons, the Mann-Whitney *U* test was used. Significances were defined as follows: *$P < 0.05$; **$P < 0.01$; ***$P < 0.001$; ****$P < 0.0001$.

(n = 46) and Pso (n = 37) samples. Higher delta Ct values represent a lower expression. Statistical significance was determined using one-way ANOVA and the Tukey's multiple comparisons tests, highlighting no significant difference in expression between macro- and microbiopsies. Significance between other comparisons are given in Supplementary Table S2a. (**i**) MC probabilities for psoriasis in macrobiopsy and microbiopsy. AD, atopic dermatitis; ma, macrobiopsy; MC, molecular classifier; mi, microbiopsy; *P*adj, adjusted *P* value; PC, principal component; PCA, principal component analysis; Pso, psoriasis.

Table 1. Patient Characteristics

	n	Age		n	Age
Pso (n = 27)			AD (n = 29)		
M	20	49.7 ± 12.89 [43.67; 55.73]	m	14	47.93 ± 25.83 [33.01; 62.84]
F	7	65.86 ± 10.12 [56.49; 75.22]	f	15	55.67 ± 29.08 [39.56; 71.77]
PG (n = 5)			NE (n = 21)		
M	2	36.5 ± 7.78 [−33.38; 106.4]	m	10	62.6 ± 15.32 [51.64; 73.56]
F	3	40.33 ± 36.86 [−51.22; 131.9]	f	11	72.27 ± 13.55 [63.7; 81.38]
GPP (n = 2)			DHE (n = 4)		
M	1	55−60	m	1	70−75
F	1	25−30	f	3	55 ± 19.29 [7.09; 102.9]
PP (n = 1)			HRE (n = 3)		
F	1	40−45	m	1	60−65
			f	2	70 ± 21.21 [−120.6; 260.6]
PPP (n = 3)			Unclear cases (n = 14)		
M	2	42 ± 9.9 [−46.94; 130.9]	m	8	56.88 ± 14.28 [44.94; 68.81]
F	1	45−50	f	6	66 ± 10.71 [54.76; 77.24]

Abbreviations: AD, atopic dermatitis; DHE, dyshidrotic eczema; f, female; GPP, generalized pustular psoriasis; HRE, hyperkeratotic-rhagadiform eczema; m, male; NE, nummular eczema; PG, psoriasis guttata; PP, psoriasis palmoplantaris; PPP, psoriasis pustulosa palmoplantaris; Pso, psoriasis.

Data availability statement

Generated data and codes can be accessed through Gene Expression Omnibus (GSE223799).

ORCIDs

Felix Fischer: http://orcid.org/0000-0001-8718-7952
Anais Doll: http://orcid.org/0000-0002-5988-5152
Deniz Uereyener: http://orcid.org/0000-0003-4952-3868
Sophie Roenneberg: http://orcid.org/0000-0003-3252-1700
Christina Hillig: http://orcid.org/0000-0001-7447-547X
Lucca Weber: http://orcid.org/0000-0002-4100-920X
Verena Hackert: http://orcid.org/0000-0001-9824-3876
Martin Meinel: http://orcid.org/0000-0002-4042-6247
Ali Farnoud: http://orcid.org/0000-0002-9298-5497
Peter Seiringer: http://orcid.org/0000-0001-6332-3323
Jenny Thomas: http://orcid.org/0000-0002-6386-7352
Philipp Anand: http://orcid.org/0000-0003-2365-4325
Larissa Graner: http://orcid.org/0000-0003-0826-3211
Franziska Schlenker: http://orcid.org/0000-0003-2082-1677
Roland Zengerle: http://orcid.org/0000-0001-5348-2216
Pontus Jonsson: http://orcid.org/0000-0002-5953-7318
Manja Jargosch: http://orcid.org/0000-0001-6051-4036
Fabian J. Theis: http://orcid.org/0000-0002-2419-1943
Carsten B. Schmidt-Weber: http://orcid.org/0000-0002-3203-8084
Tilo Biedermann: http://orcid.org/0000-0002-5352-5105
Michael Howell: http://orcid.org/0000-0002-7409-7883
Kristian Reich: http://orcid.org/0000-0001-5248-4332
Kilian Eyerich: http://orcid.org/0000-0003-0094-2674
Michael Menden: http://orcid.org/0000-0003-0267-5792
Natalie Garzorz-Stark: http://orcid.org/0000-0002-7409-7883
Felix Lauffer: http://orcid.org/0000-0002-1992-2836
Stefanie Eyeric: http://orcid.org/0000-0002-1166-2355

CONFLICT OF INTEREST

FJT consults for Immunai Inc, Singularity Bio B.V., CytoReason Ltd, and Omniscope Ltd, and has ownership interests in Dermagnostix GmbH and Cellarity. MH was an employee and shareholder in DermTech at the time of the study. KR is cofounder and shareholder of Moonlake Immunotherapeutics and Dermagnostix R&D and a shareholder of Dermagnostix. KR has served as an advisor and/or paid speaker for and/or participated in clinical trials sponsored by AbbVie, Almirall, Amgen, Boehringer Ingelheim, Bristol-Myers Squibb, Celgene, Forward Pharma, Gilead, Galderma, Janssen-Cilag, Kyowa Kirin, Leo, Eli Lilly, Medac, Novartis, Ocean Pharma, Pfizer, Sanofi, UCB. KE, NGS, and SE are the founders and shareholders of Dermagnostix and Dermagnostix R&D. KE is an inventor on the patent "differential diagnosis of psoriasis and eczema." FL received speaker's and/or consulting fees from Janssen-Cilag Pharma, Amgen, UCB Pharma, Boehringer Ingelheim, Bristol-Myers-Squibb, Union Therapeutics, AbbVie, Novartis Pharma, LEO Pharma, Eli Lilly, Roche, Sanofi, Almirall, and Pfizer. The remining authors state no conflict of interest.

ACKNOWLEDGMENTS

The authors thank Kerstin Weber for excellent technical support and the Biobank Biederstein for patient samples. This work was supported by the Medical Valley Award, the IGSSE graduate school, the GRK2668, and the Munich School for Data Science.

AUTHOR CONTRIBUTIONS

Conceptualization: NGS, FL, SE, MiM, KE, CH; Data Analysis: FF, AD, DU, CH, MiM, KE AF; Funding Acquisition: NGS, SE, FL; Investigation: AD, PA, SR, PS, JT, LG, FS, MJ, FL, NGS, PJ, SE; Tape Study: LW, VH; Resources: CBSW, TB, FJT, RZ; Supervision: AF, MiM, SE, FL; Writing and Editing: FF, AD, DU, SR, CH, LW, VH, MaM, AF, PS, JT, PA, LG, FS, RZ, PJ, MJ, FJT, CBSW, TB, MH, KR, KE, MiM, NGS, FL, SE

SUPPLEMENTARY MATERIAL

Supplementary material is linked to the online version of the paper at www.jidonline.org, and at https://doi.org/10.1016/j.jid.2023.02.015.

REFERENCES

Andersson AM, Sølberg J, Koch A, Skov L, Jakasa I, Kezic S, et al. Assessment of biomarkers in pediatric atopic dermatitis by tape strips and skin biopsies. Allergy 2022;77:1499−509.

Bentz P, Eyerich K, Weber K, Kluge L, Ofenloch R, Weisshaar E. [Cohort study for long-term follow-up of patients in whom the so-called "molecular classifier" is used to distinguish eczema from psoriasis : background and implementation]. Hautarzt 2021;72:354−7.

Brunner PM, Pavel AB, Khattri S, Leonard A, Malik K, Rose S, et al. Baseline IL-22 expression in patients with atopic dermatitis stratifies tissue responses to fezakinumab. J Allergy Clin Immunol 2019;143:142−54.

Bylund S, von Kobyletzki LB, Svalstedt M, Svensson Å. Prevalence and incidence of atopic dermatitis: A systematic review. Acta Derm Venereol 2020;100:adv00160.

Churiso G, van Henten S, Cnops L, Pollmann J, Melkamu R, Lemma M, et al. Minimally invasive microbiopsies as an improved sampling method for the diagnosis of cutaneous leishmaniasis. Open Forum Infect Dis 2020;7:ofaa364.

Garzorz-Stark N, Krause L, Lauffer F, Atenhan A, Thomas J, Stark SP, et al. A novel molecular disease classifier for psoriasis and eczema. Exp Dermatol 2016;25:767−74.

Grazia G, Penna I, Perotti V, Anichini A, Tassi E. Towards combinatorial targeted therapy in melanoma: from pre-clinical evidence to clinical application (review). Int J Oncol 2014;45:929−49.

Hadeler E, Mosca M, Hong J, Brownstone N, Liao W, Bhutani T. Innovations in translational research in dermatology: minimally invasive methods for biosample acquisition. Dermatol Online J 2021;27. https://doi.org/10.5070/D3271055695.

He H, Bissonnette R, Wu J, Diaz A, Saint-Cyr Proulx E, Maari C, et al. Tape strips detect distinct immune and barrier profiles in atopic dermatitis and psoriasis. J Allergy Clin Immunol 2021;147:199–212.

Kolesnik M, Franke I, Lux A, Quist SR, Gollnick HP. Eczema in Psoriatico: an important differential diagnosis between chronic allergic contact dermatitis and psoriasis in palmoplantar localization. Acta Derm Venereol 2018;98:50–8.

Levine D, Fisher DE. Current status of diagnostic and prognostic markers in melanoma. Methods Mol Biol 2014;1102:177–97.

Mikhaylov D, Del Duca E, Olesen CM, He H, Wu J, Ungar B, et al. Transcriptomic profiling of tape-strips from moderate to severe atopic dermatitis patients treated with dupilumab. Dermatitis 2021;32:S71–80.

Noda S, Krueger JG, Guttman-Yassky E. The translational revolution and use of biologics in patients with inflammatory skin diseases. J Allergy Clin Immunol 2015;135:324–36.

Poh SE, Koh WLC, Lim SYD, Wang ECE, Yew YW, Common JEA, et al. Expression of Staphylococcus aureus virulence factors in atopic dermatitis. JID Innov 2022;2:100130.

Quaranta M, Knapp B, Garzorz N, Mattii M, Pullabhatla V, Pennino D, et al. Intraindividual genome expression analysis reveals a specific molecular signature of psoriasis and eczema. Sci Transl Med 2014;6:244ra90.

Renert-Yuval Y, Thyssen JP, Bissonnette R, Bieber T, Kabashima K, Hijnen D, et al. Biomarkers in atopic dermatitis—a review on behalf of the International Eczema Council. J Allergy Clin Immunol 2021;147:1174–90.e1.

Stoffel E, Maier H, Riedl E, Brüggen MC, Reininger B, Schaschinger M, et al. Analysis of anti-tumour necrosis factor-induced skin lesions reveals strong T helper 1 activation with some distinct immunological characteristics. Br J Dermatol 2018;178:1151–62.

Thyssen JP, Johansen JD, Linneberg A, Menné T. The epidemiology of hand eczema in the general population–prevalence and main findings. Contact Dermatitis 2010;62:75–87.

Tizek L, Schuster B, Gebhardt C, Reich K, von Kiedrowski R, Biedermann T, et al. Molecular diagnostics in dermatology: an online survey to study usage, obstacles and requirements in Germany. J Dtsch Dermatol Ges 2022;20:287–95.

Usher-Smith JA, Emery J, Kassianos AP, Walter FM. Risk prediction models for melanoma: a systematic review. Cancer Epidemiol Biomarkers Prev 2014;23:1450–63.

Vena GA, Altomare G, Ayala F, Berardesca E, Calzavara-Pinton P, Chimenti S, et al. Incidence of psoriasis and association with comorbidities in Italy: a 5-year observational study from a national primary care database. Eur J Dermatol 2010;20:593–8.

Yamada M, Melville E, Cowin AJ, Prow TW, Kopecki Z. Microbiopsy-based minimally invasive skin sampling for molecular analysis is acceptable to epidermolysis bullosa Simplex patients where conventional diagnostic biopsy was refused. Skin Res Technol 2021;27:461–3.

This work is licensed under a Creative Commons Attribution-NonCommercial-NoDerivatives 4.0 International License. To view a copy of this license, visit http://creativecommons.org/licenses/by-nc-nd/4.0/

SUPPLEMENTARY MATERIALS AND METHODS

The molecular classifier supports diagnostic decision making in patients with inconsistent diagnosis

Patient 43 (Supplementary Figure S1a and b [1]), a woman close to the age of 80 years, developed shortly after a respiratory infection itchy, pustular reddening overall the whole body. Bacterial or viral infections were not detected. Extensive lesional skin at the thigh and knee was surgically excised. Histologically, the lesions presented with infiltration of neutrophils and isolated eosinophils, signs of spongiosis, and in part, parakeratosis. The patient was diagnosed with psoriasis pustulosa; however, acute generalized exanthematic pustulosis could not be ruled out. In fact, psoriasis pustulosa and acute generalized exanthematic pustulosis can hardly be distinguished by a classical histologic examination. Our formalin-fixed and paraffin-embedded–based molecular classifier (MC) assigned this patient a probability of psoriasis of 74.49%. After initiation of ixekizumab, the skin status of this patient improved, supporting the MC-based classification (Supplementary Figure S1b [1]).

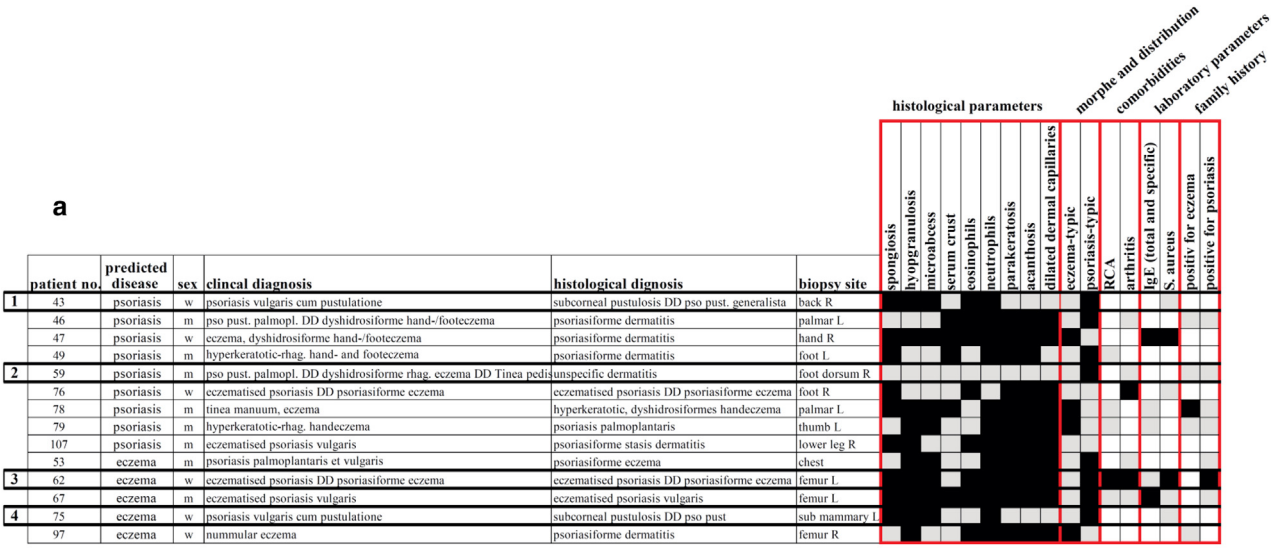
Patient 59 (Supplementary Figure S1a and b [2]), a man in mid-60s, presented in the clinic with reddish, hyperkeratotic, scaly, and itchy skin lesions at both palmae, accompanied by erythematous, heavily infiltrated plaques at the back, capillitium, and retroauricular. Histopathologic examination showed psoriasiform acanthosis, hyperparakeratosis, a lymphocytic infiltrate, and isolated plasma cells, leading to the diagnosis of psoriasiform perivascular dermatitis, while clinically, the diagnostics were in favor for psoriasis. The formalin-fixed and paraffin-embedded–based MC assigned a probability for psoriasis of 99.53%. Skin lesions on the palms and body cleared after 6 months of methotrexate therapy (Supplementary Figure S1b [2]).

Patient 62 (Supplementary Figure S1a and b [3]), a man at the end of his 60s, presented at the clinic with confluent, erythematous, crude-lamellar, scaly plaques at both palmae. Histologically, extended hyperparakeratosis, serum crusts, psoriasiform epidermis hyperplasia combined with spongiosis, and a linear lymphocytic infiltrate in the absence of neutrophils and eosinophils were described, leading to the diagnosis of hyperkeratotic, in part dyshidrotic hand eczema. The formalin-fixed and paraffin-embedded–based MC assigned this patient a probability for psoriasis of 8.25% and thereby a high likelihood of an underlying eczematous disease. Treatment with topical corticosteroids and alitretinoin improved the skin lesions, supporting the MC-based classification (Supplementary Figure S1b [3]).

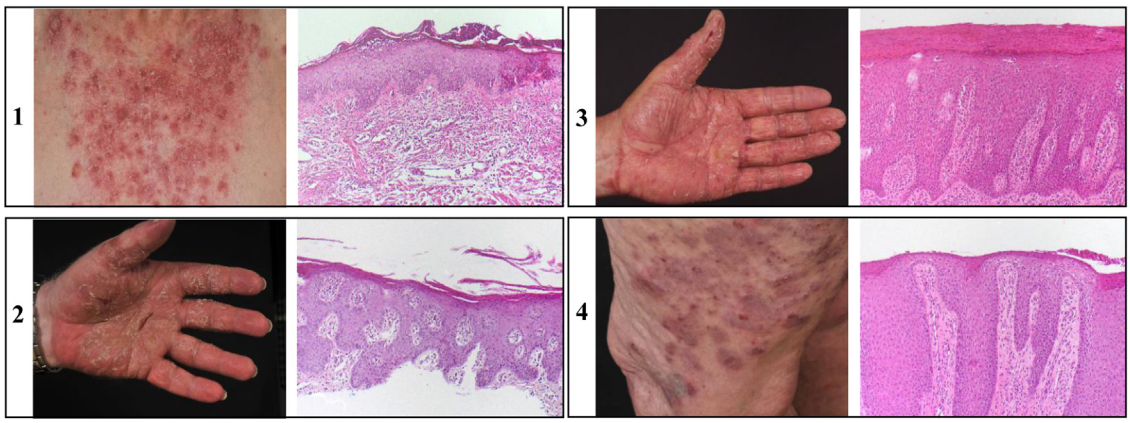
Patient 75 (Supplementary Figure S1a and b [4]), a woman at the beginning of her 60s, has been suffering for years under recurrent itchy, sharply demarcated erythematous plaques, with in part lamellar scales and excoriations as clinically seen in both psoriasis and eczema variants. Histologically, a psoriasiform hyperplasia of the epidermis was found in combination with hyperparakeratosis, hypogranulosis, elongated rete-ridges, papillomatosis, and focal spongiosis in the upper epidermis layers was found. A perivascular dense lymphocytic infiltrate with an absence of neutrophils and eosinophils was identified. The patient was diagnosed with nummular eczema. This is supported also by the formalin-fixed and paraffin-embedded–based MC that assigned a probability of 18.29% to this patient (Supplementary Figure S1b [4]) and skin lesions improved with topical corticosteroids and UVB phototherapy.

a

	patient no.	predicted disease	sex	clincal diagnosis	histological dignosis	biopsy site
1	43	psoriasis	w	psoriasis vulgaris cum pustulatione	subcorneal pustulosis DD pso pust. generalista	back R
	46	psoriasis	m	pso pust. palmopl. DD dyshidrosiforme hand-/footeczema	psoriasiforme dermatitis	palmar L
	47	psoriasis	w	eczema, dyshidrosiforme hand-/footeczema	psoriasiforme dermatitis	hand R
	49	psoriasis	m	hyperkeratotic-rhag. hand- and footeczema	psoriasiforme dermatitis	foot L
2	59	psoriasis	m	pso pust. palmopl. DD dyshidrosiforme rhag. eczema DD Tinea pedis	unspecific dermatitis	foot dorsum R
	76	psoriasis	w	eczematised psoriasis DD psoriasiforme eczema	eczematised psoriasis DD psoriasiforme eczema	foot R
	78	psoriasis	m	tinea manuum, eczema	hyperkeratotic, dyshidrosiformes handeczema	palmar L
	79	psoriasis	m	hyperkeratotic-rhag. handeczema	psoriasis palmoplantaris	thumb L
	107	psoriasis	m	eczematised psoriasis vulgaris	psoriasiforme stasis dermatitis	lower leg R
	53	eczema	m	psoriasis palmoplantaris et vulgaris	psoriasiforme eczema	chest
3	62	eczema	w	eczematised psoriasis DD psoriasiforme eczema	eczematised psoriasis DD psoriasiforme eczema	femur L
	67	eczema	m	eczematised psoriasis vulgaris	eczematised psoriasis vulgaris	femur L
4	75	eczema	w	psoriasis vulgaris cum pustulatione	subcorneal pustulosis DD pso pust	sub mammary L
	97	eczema	w	nummular eczema	psoriasiforme dermatitis	femur R



b



Supplementary Figure S1. The FFPE-based MC is able to support diagnosis of unclear cases. (**a**) The FFPE-based MC was applied on clinically and histologically challenging cases of patients with a suspected diagnosis of psoriasis or eczema and subtypes of both diseases (n = 14). Given patient numbers represent numerical numbering and not biobank IDs. Black = yes, gray = no, white = not determined. Numbers 1−4 correspond to patients 1−4 shown in (b). (**b**) Clinical pictures and histological H&E stainings of four selected patients (1−4) with unclear initial diagnosis that were assigned a probability of psoriasis (1−2) or eczema (3−4) by the FFPE-based MC. FFPE, formalin-fixed and paraffin-embedded; ID, identification; MC, molecular classifier.

Supplementary Table S2. Significant Differences between Gene Expression in Macrobiopsies Versus Microbiopsies and FFPE Versus Tape Strip PCR Results

a. Significances Macrobiopsy Versus Microbiopsy

Tukey's Multiple Comparisons Test	Mean Diff	95% CI of Diff	Summary	Adjusted *P*-Value
AD CCL27 macro versus AD CCL27 micro	−0.292	−1.859 to 1.276	ns	0.9991
AD CCL27 macro versus AD NOS22 macro	−8.997	−10.56 to −7.429	****	<0.0001
AD CCL27 macro versus AD NOS2 micro	−9.495	−11.06 to −7.928	****	<0.0001
AD CCL27 macro versus Pso CCL27 macro	−2.741	−4.739 to −0.7429	**	0.0011
AD CCL27 macro versus Pso CCL27 micro	−2.734	−4.732 to −0.7360	**	0.0011
AD CCL27 macro versus Pso NOS2 macro	−3.318	−5.316 to −1.320	****	<0.0001
AD CCL27 macro versus Pso NOS2 micro	−2.287	−4.285 to −0.2887	*	0.0131
AD CCL27 micro versus AD NOS22 macro	−8.705	−10.27 to −7.138	****	<0.0001
AD CCL27 micro versus AD NOS2 micro	−9.204	−10.77 to −7.636	****	<0.0001
AD CCL27 micro versus Pso CCL27 macro	−2.450	−4.448 to −0.4514	**	0.0056
AD CCL27 micro versus Pso CCL27 micro	−2.443	−4.441 to −0.4445	**	0.0059
AD CCL27 micro versus Pso NOS2 macro	−3.027	−5.025 to −1.028	***	0.0002
AD CCL27 mcro versus Pso NOS2 micro	−1.995	−3.993 to 0.002897	ns	0.0506
AD NOS22 macro versus AD NOS2 mcro	−0.499	−2.066 to 1.069	ns	0.9769
AD NOS22 macro versus Pso CCL27 macro	6.256	4.258 to 8.254	****	<0.0001
AD NOS22 macro versus Pso CCL27 micro	6.263	4.265 to 8.261	****	<0.0001
AD NOS22 macro versus Pso NOS2 macro	5.679	3.681 to 7.677	****	<0.0001
AD NOS22 macro veruss Pso NOS2 micro	6.710	4.712 to 8.708	****	<0.0001
AD NOS2 micro veruss Pso CCL27 macro	6.754	4.756 to 8.753	****	<0.0001
AD NOS2 micro versus Pso CCL27 micro	6.761	4.763 to 8.759	****	<0.0001
AD NOS2 micro versus Pso NOS2 macro	6.177	4.179 to 8.176	****	<0.0001
AD NOS2 micro versus Pso NOS2 micro	7.209	5.210 to 9.207	****	<0.0001
Pso CCL27 macro versus Pso CCL27 micro	0.007	−2.344 to 2.358	ns	>0.9999
Pso CCL27 macro versus Pso NOS2 macro	−0.577	−2.928 to 1.774	ns	0.995
Pso CCL27 macro versus Pso NOS2 micro	0.454	−1.897 to 2.806	ns	0.9989
Pso CCL27 micro versus Pso NOS2 macro	−0.584	−2.935 to 1.767	ns	0.9947
Pso CCL27 micro versus Pso NOS2 micro	0.447	−1.904 to 2.799	ns	0.999
Pso NOS2 macro versus Pso NOS2 micro	1.031	−1.320 to 3.383	ns	0.8784

b. Significances FFPE Versus Tape Strips

Tukey's Multiple Comparisons Test	Mean Diff	95.00% CI of Diff	Summary	Adjusted *P*-Value
AD CCL27 FFPE versus AD CCL27 Tape	−0.747	−3.211 to 1.717	ns	0.9831
AD CCL27 FFPE versus AD NOS2 FFPE	−18.870	−20.16 to −17.58	****	<0.0001
AD CCL27 FFPE versus AD NOS2 Tape	−15.110	−17.57 to −12.64	****	<0.0001
AD CCL27 FFPE versus Pso CCL27 FFPE	−2.244	−3.718 to −0.7688	***	0.0001
AD CCL27 FFPE versus Pso CCL27 Tape	−2.906	−5.271 to −0.5408	**	0.0053
AD CCL27 FFPE versus Pso NOS2 FFPE	−2.205	−3.776 to −0.6332	***	0.0007
AD CCL27 FFPE versus Pso NOS2 Tape	0.722	−1.643 to 3.087	ns	0.9824
AD CCL27 tape versus AD NOS2 FFPE	−18.120	−20.59 to −15.66	****	<0.0001
AD CCL27 tape versus AD NOS2 tape	−14.360	−17.60 to −11.12	****	<0.0001
AD CCL27 tape versus Pso CCL27 FFPE	−1.497	−4.062 to 1.069	ns	0.6313
AD CCL27 tape versus Pso CCL27 tape	−2.159	−5.322 to 1.004	ns	0.4256
AD CCL27 tape versus Pso NOS2 FFPE	−1.458	−4.080 to 1.165	ns	0.6872
AD CCL27 tape versus Pso NOS2 tape	1.469	−1.694 to 4.632	ns	0.8468
AD NOS2 FFPE versus AD NOS2 tape	3.763	1.299 to 6.227	***	0.0001
AD NOS2 FFPE versus Pso CCL27 FFPE	16.630	15.15 to 18.10	****	<0.0001
AD NOS2 FFPE versus Pso CCL27 tape	15.960	13.60 to 18.33	****	<0.0001
AD NOS2 FFPE versus Pso NOS2 FFPE	16.660	15.09 to 18.24	****	<0.0001
AD NOS2 FFPE versus Pso NOS2 tape	19.590	17.23 to 21.96	****	<0.0001
AD NOS2 tape versus Pso CCL27 FFPE	12.860	10.30 to 15.43	****	<0.0001
AD NOS2 tape versus Pso CCL27 tape	12.200	9.037 to 15.36	****	<0.0001
AD NOS2 tape versus Pso NOS2 FFPE	12.900	10.28 to 15.52	****	<0.0001
AD NOS2 tape versus Pso NOS2 tape	15.830	12.67 to 18.99	****	<0.0001
Pso CCL27 FFPE versus Pso CCL27 tape	−0.662	−3.134 to 1.809	ns	0.9919
Pso CCL27 FFPE versus Pso NOS2 FFPE	0.039	−1.687 to 1.766	ns	>0.9999
Pso CCL27 FFPE versus Pso NOS2 tape	2.966	0.4946 to 5.437	**	0.0072

(*continued*)

Supplementary Table S2. Continued

b. Significances FFPE Versus Tape Strips

Tukey's Multiple Comparisons Test	Mean Diff	95.00% CI of Diff	Summary	Adjusted *P*-Value
Pso CCL27 tape versus Pso NOS2 FFPE	0.702	−1.828 to 3.231	ns	0.99
Pso CCL27 tape versus Pso NOS2 tape	3.628	0.5418 to 6.715	**	0.0093
Pso NOS2 FFPE versus Pso NOS2 tape	2.927	0.3967 to 5.457	*	0.0113

Abbreviations: AD, atopic dermatitis; CI, confidence interval; Diff, difference; FFPE, formalin-fixed and paraffin-embedded; ns, nonsignificant; Pso, psoriasis.

*$P < 0.05$; **$P < 0.01$; ***$P < 0.001$; ****$P < 0.0001$.

Supplementary Table S3. Primers, Probes, and Kits for Real-Time PCR

Method/ Marker	FFPE and Tape Strips	RNAprotect
cDNA transcription	One-step	Two-step
Real-time PCR	Hydrolysis probe	SYBR green
Primer/probes		
NOS2	fw: 5′- TTCCTGGTTTGACTGTCCTTACC-3′ rev: 5′-TTTCACTGTGGGGCTTGC-3′ probe: 5′-CGGGGAGGCAGTGCAGCCAGC-3′	fw: 5′-ATCTGCAGACACGTGCGTTA-3′ rev: 5′-TGATGGCCGACCTGATGTTG -3′
CCL27	fw: 5′- ACCCTACAGCAGCATTCCTAC-3′ rev: 5′- AGCTTGTCTGAGAGTGGCTTTC-3′ probe: 5′-ACCCAGCACTGCCTGCTGTACTCAGCTC-3′	Fw: 5′-CCCTACAGCAGCATTCCTAC-3′ rev: 5′-GTAGAGCTGAGTACAGCAGGC-3′
TBP	fw: 5′- ATGGATCAGAACAACAGCCTGC-3′ rev: 5′- CATTGGACTAAAGATAGGGATTCCG-3′ probe: 5′- TCAGGGCTTGGCCTCCCCTCAGGGTGCC-3′	
SDHAF2	fw: 5′- CGGTGTCTACAGTGTTCTCGAC-3′ rev: 5′- GATGTCACACTGAGCAAAGGAG-3′ probe: 5′-CGCTGATGCTTGCTCTGTCAAGGCACAGCC-3′	
18S		fw: 5′-GTAACCCGTTGAACCCCATTC-3′ rev: 5′-CGCACTTACTGGGAATTCCTC-3′

Abbreviations: fw, forward; rev, reverse.